Mechanics of Time-Dependent Materials
https://doi.org/10.1007/s11043-023-09640-w

RESEARCH

Tailorable non-linear viscoelastic behavior of hydrogels

Nada Qari[1] · Zhaoqiang Song[2] · Hamed Hosseini-Toudeshki[2] · Chenghai Li[2] · Shengqiang Cai[1,2]

Received: 31 May 2023 / Accepted: 21 September 2023
© The Author(s), under exclusive licence to Springer Nature B.V. 2023

Abstract
In this work, we investigate the viscoelastic properties of hydrogels through stress relaxation experiments to better understand the force-dependent dynamics of these materials with the aspiration of expanding their application envelope within the biomedical field and beyond. We experimentally studied the viscoelastic behavior of 4 different types of hydrogels: covalently crosslinked polyacrylamide (PAAm), covalently crosslinked PAAm network immersed in a viscous alginate solution, ionically crosslinked alginate along with crosslinked PAAm-alginate double network. Through our investigations, we demonstrate that we can tailor the viscoelasticity of a covalently bonded PAAm network by tuning the viscosity of the solution in the gel. Moreover, based on the stress relaxation test of ionically crosslinked alginate gel and the double network gel, we have revealed the quantitative correlation between the ionic bond dissociation and force-dependent viscoelastic behavior of gels containing ionic crosslinks.

Keywords Hydrogels · Viscoelasticity · Force-dependent · Stress relaxation · Rheological model · Relaxation time

1 Introduction

Hydrogels are a special kind of polymer-based gel composed of a three-dimensional hydrophilic polymer network in which a large amount of water is interposed (Nakayama et al. 2004). Depending on the type of crosslinkers, hydrogels can be categorized into covalently (or chemically) crosslinked gels and ionically (or physically) crosslinked gels (Tang et al. 2016). In a hydrogel, hydrophilic polymers can retain a large amount of water, and this gives hydrogels unique proprieties that make them suitable for many applications in the biomedical field, active devices, soft robots, and environmental engineering (Nakayama et al. 2004; Sun et al. 2012). Examples of the applications of hydrogels include scaffolds for tissue engineering, vehicles for drug delivery, actuators for optics and fluidics, and model extracellular matrices for biological studies (Sun et al. 2012).

✉ S. Cai
shqcai@ucsd.edu

1 Program of Materials Science and Engineering, University of California San Diego, La Jolla, CA 92093, USA

2 Department of Mechanical and Aerospace Engineering, University of California San Diego, La Jolla, CA 92093, USA

Published online: 04 October 2023

Inspired by nature, and since most tissues found in animals and plants are composed of hydrogels (Bai et al. 2019), many synthetic hydrogels have been designed to mimic the behavior of natural tissue. Some of the most common polymers used include alginate, a naturally occurring polysaccharide co-polymer found in brown seaweed that is composed of irregular block arrangements of α-L-guluronate (G-Block) and β-D-mannuronate (M-Block) (Agulhon et al. 2012). Another commonly used polymer is polyacrylamide (PAAm), which is a synthetic linear polymer often composed of acrylamide monomer units or a combination of acrylamide and acrylic acid (Bai et al. 2019).

As stated previously, hydrogels are composed of long polymer chains that constantly interact within the gel's network (Ligia and Deodato 2009; Drozdov and Kalamkarov 1996). This often leads to complex viscoelastic behavior, which may result from various microscopic processes, including sliding between polymer chains, temporary bond formation and breakage etc. (Ligia and Deodato 2009; Drozdov and Kalamkarov 1996; Green and Tobolsky 1946). Recent studies have found that the viscoelasticity of soft tissues plays an important role in many biological processes, including regulating cell behaviors, differentiation, and malignancy (Nam et al. 2016; Chaudhuri et al. 2016; Guimarães et al. 2020; Storm et al. 2005). Consequently, lots of efforts have been dedicated to developing hydrogels with tunable viscoelasticity that closely match the behavior of biological tissues (Chaudhuri 2017; Agarwal et al. 2021). Moreover, theoretical frameworks have been formulated that highlight the dynamic, time-dependent behavior of self-healing gels (Long et al. 2014), transient polymer networks, and dual crosslink gels (Shen et al. 2021; Meng et al. 2016; Mayumi et al. 2013) all of which have significantly advanced the biomedical applications of hydrogels.

In the current study, we aim to conduct systematic investigations of the viscoelastic behavior of hydrogels. Due to the low viscosity of water, the resistance to the movement of the polymer chains in a hydrogel is very small. As a result, covalently crosslinked hydrogels typically exhibit hyperelastic behavior with little viscous effects or mechanical dissipation. In contrast, for an ionically crosslinked hydrogel such as Ca^{2+} crosslinked alginate, the ionic bond can be unzipped by external forces, which is a rate-dependent process and can dissipate energy. As a result, an ionically crosslinked hydrogel usually exhibits significant viscoelastic properties. Though the viscoelasticity of an ionically crosslinked hydrogel has often been ascribed to the ionic debonding process, according to our knowledge, quantitative analyses correlating the macroscopically viscoelastic behavior of hydrogels with the microscopic ionic debonding process has yet to be done. Moreover, it is reasonable to expect that the dynamic ionic debonding process in a hydrogel is force-dependent. Therefore, the time scales associated with the viscoelastic behaviors of a hydrogel should also be dependent on its external load. Recent work has also shown that the load-dependent stress relaxation of hydrogels can profoundly affect their fracturing process (Wang et al. 2023). However, in most previous studies, the time scale (s) associated with the viscoelasticity of ionically crosslinked hydrogels are assumed to be constant.

In this work, we conduct stress relaxation experiments to systematically study the viscoelastic behavior of four different hydrogels: covalently crosslinked PAAm, covalently crosslinked PAAm network immersed in a viscous alginate solution, ionically crosslinked alginate, and crosslinked PAAm-alginate double network. We found that we can tailor the viscoelastic behavior of a covalently crosslinked PAAm hydrogel by increasing the viscosity of the aqueous solution in which the polymer network is immersed. We have also demonstrated that the macroscopically measured force-dependent viscoelastic behavior of ionically crosslinked alginate gel and PAAm-alginate double network gel can be quantitatively interpreted by the microscopic ionic debonding process in the gel.

2 Hydrogel synthesis

The hydrogels were prepared by following the previous work (Sun et al. 2012). Briefly, the 2 wt% alginate gel was prepared by mixing 2.5 g of medium viscosity alginic acid sodium salt from brown algae (Sigma-Aldrich A2033) with 122.5 g of deionized water where 2.5 vol% Calcium Sulfate dihydrate ($CaSO_4 \cdot 2H_2O$, Sigma-Aldrich C3771) was used as a crosslinker. The 8 wt% PAAm gel was prepared by mixing 10 g of Acrylamide (Sigma-Aldrich 79-06-1) with 115 g of deionized water where 0.96 vol% N,N′-Methylenebisacrylamide (2 wt% MBAA, Sigma-Aldrich 146072) was used as a crosslinker, 1.53 vol% Ammonium persulfate (0.27 M APS, Sigma-Aldrich A3678) was used as an initiator and 0.055 vol% Tetramethylethylenediamine (TEMED, Sigma-Aldrich T9281) was used as a catalyst.

The double network hydrogel was fully crosslinked and prepared by homogenously mixing the 2 wt% alginate and 8 wt% PAAm solutions while using the same amount of $CaSO_4 \cdot 2H_2O$, MBAA, APS and TEMED. The immersion of a covalently crosslinked PAAm network in a viscous alginate solution was achieved by using the same procedure for the double network. However, the $CaSO_4 \cdot 2H_2O$ ionic crosslinker was eliminated to keep the alginate chains in linear form.

3 Experimental methods

3.1 Sample preparation

A 30 mL syringe was used as a mold to create cylindrical-shaped samples for compression testing. After 24 hours of crosslinking 10 mL of the desired gel, the cylindrical-shaped sample was removed from the mold where the average value of the diameter was equal to 22.5 mm, and the diameter-to-length ratio was kept at 1:1. After that, the sample was fully immersed in a silicon oil bath to prevent water evaporation throughout the test.

3.2 Stress relaxation test

Using the 10 N load cell on the Instron (Model # 3345), a compressive strain was applied on each hydrogel and was held constant for 3 hours. This setup (Fig. 1) was used to conduct different compression experiments on each hydrogel, starting with 5% compressive strain followed by 10%, 15%, and 20% compressive strain.

In each experiment, the time to reach maximum compressive strain was equal to 2 seconds through adjusting the compressive strain rate. For instance, a 2.5%/s rate was used during the 5% compression test, while 5%/s, 7.5%/s, and 10%/s were used during the 10%, 15%, and 20% compression tests, respectively. Throughout the experiment, the stress was recorded as a function of time to characterize the stress relaxation behavior of the prepared hydrogels.

4 Model of non-linear viscoelasticity of hydrogels

A rheological model of springs and dashpots can represent the viscoelastic relaxation of hydrogels. Here, we adopt a simple rheological model of three parallel units: one consists of a single spring, and the other two consist of a spring and a dashpot, as shown in Fig. 2.

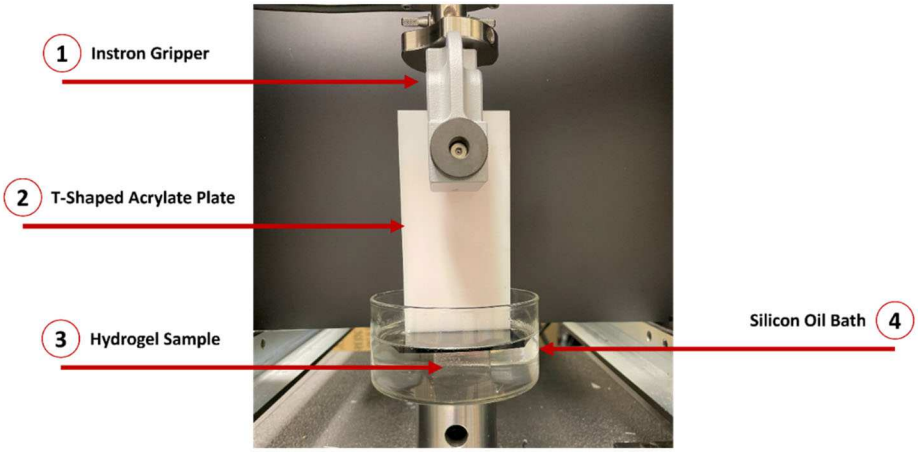

Fig. 1 The 10 N Instron load cell was used to apply a compressive strain on the sample, which was held constant for 3 hours where the sample was fully immersed in a silicon oil bath to prevent the evaporation of water throughout the experiment

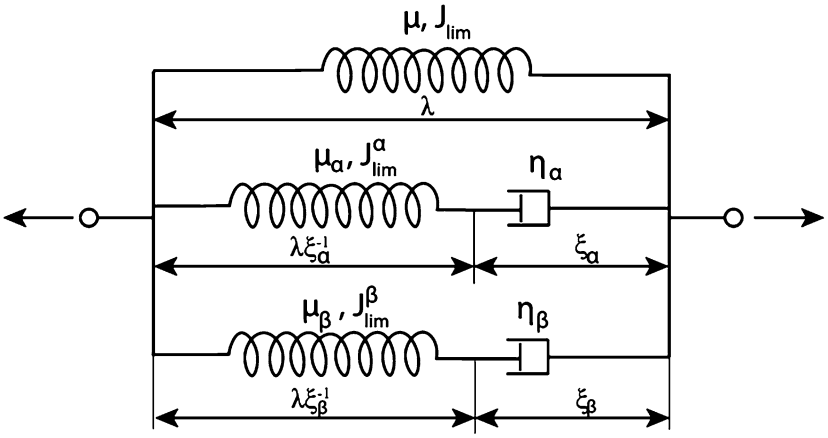

Fig. 2 Rheological model used to obtain fitting parameters based on experimentally observed stress relaxation behavior, where μ, μ_α, and μ_β are the shear moduli for the springs. The viscosity of the dashpots is described by η_α and η_β. λ is the applied stretch. ξ_α and ξ_β are used to describe dashpot deformation under uniaxial compression, while the J_{lim}, J^{α}_{lim} and J^{β}_{lim} values represent the chain extensibility of the springs

This rheological model has two relaxation times, which should provide better fitting results than the model only containing one relaxation time. In the discussion later, we found the two relaxation times are well separated, and we will be mainly focused on studying the first (primary) relaxation time.

In a principal coordinate, for a single spring unit, the state of deformation can be described by three principal stretches of the hydrogel: λ_1, λ_2 and λ_3; however, for the two spring and dashpot units, the state of elastic deformation is given by $\lambda_1\xi_{\alpha 1}^{-1}$, $\lambda_2\xi_{\alpha 2}^{-1}$, $\lambda_3\xi_{\alpha 3}^{-1}$, $\lambda_1\xi_{\beta 1}^{-1}$, $\lambda_2\xi_{\beta 2}^{-1}$, and $\lambda_3\xi_{\beta 3}^{-1}$, where $\xi_{\alpha 1}$, $\xi_{\alpha 2}$, $\xi_{\alpha 3}$, $\xi_{\beta 1}$, $\xi_{\beta 2}$, and $\xi_{\beta 3}$, are used to describe dashpot deformation.

For a uniaxial compression test along direction 1, we have:

$$\lambda_1 = \lambda, \tag{1}$$

$$\lambda_2 = \lambda_3 = \lambda^{-\frac{1}{2}}, \tag{2}$$

and

$$\xi_{\alpha 1} = \xi_\alpha \text{ and } \xi_{\beta 1} = \xi_\beta, \tag{3}$$

$$\xi_{\alpha 2} = \xi_{\alpha 3} = \xi_\alpha^{-\frac{1}{2}} \text{ and } \xi_{\beta 2} = \xi_{\beta 3} = \xi_\beta^{-\frac{1}{2}}. \tag{4}$$

Using the Gent model, we can define the free energy density of the gel under uniaxial compression as follows:

$$W = -\frac{\mu J_{limit}}{2} \ln\left(1 - \frac{\lambda^2 + 2\lambda^{-1} - 3}{J_{limit}}\right) - \frac{\mu_\alpha J^\alpha_{limit}}{2} \ln\left(1 - \frac{\lambda^2 \xi_\alpha^{-2} + 2\lambda^{-1}\xi_\alpha - 3}{J^\alpha_{limit}}\right) - \frac{\mu_\beta J^\beta_{limit}}{2} \ln\left(1 - \frac{\lambda^2 \xi_\beta^{-2} + 2\lambda^{-1}\xi_\beta - 3}{J^\beta_{limit}}\right). \tag{5}$$

We assume that for alginate gel and double network, $J_{limit} = J^\alpha_{limit} = J^\beta_{limit}$; while, for PAAm gel dissolved in water and immersed in alginate solution, $J_{limit} = J^\alpha_{limit} = J^\beta_{limit} = \infty$ which reduces the Gent model to the Neo-Hookean model. According to Eq. (5), the Cauchy (true) stress can be written as:

$$\begin{aligned}\sigma &= \lambda \frac{\partial W}{\partial \lambda} = \sigma + \sigma_\alpha + \sigma_\beta \\ &= \frac{\mu\left(\lambda^2 - \lambda^{-1}\right)}{1 - \frac{\lambda^2 + 2\lambda^{-1} - 3}{J_{limit}}} + \frac{\mu_\alpha\left(\lambda^2 \xi_\alpha^{-2} - \lambda^{-1}\xi_\alpha\right)}{1 - \frac{\lambda^2 \xi_\alpha^{-2} + 2\lambda^{-1}\xi_\alpha - 3}{J^\alpha_{limit}}} + \frac{\mu_\beta\left(\lambda^2 \xi_\beta^{-2} - \lambda^{-1}\xi_\beta\right)}{1 - \frac{\lambda^2 \xi_\beta^{-2} + 2\lambda^{-1}\xi_\beta - 3}{J^\beta_{limit}}},\end{aligned} \tag{6}$$

where σ is the stress on the single spring unit, while σ_α and σ_β are the stresses on the respective spring and dashpot units. The viscous behavior of the dashpots in Fig. 2 can be described by a Newtonian fluid as:

$$\frac{d\xi_\alpha}{\xi_\alpha dt} = \frac{\sigma_\alpha}{3\eta_\alpha} \text{ and } \frac{d\xi_\beta}{\xi_\beta dt} = \frac{\sigma_\beta}{3\eta_\beta}, \tag{7}$$

where η_α and η_β are the shear viscosity of the dashpots. Using the viscosity of dashpots η_α, η_β and the shear moduli of the springs μ_α, μ_β, we can obtain two relaxation times (τ):

$$\tau_1 = \frac{\eta_\alpha}{\mu_\alpha} \text{ and } \tau_2 = \frac{\eta_\beta}{\mu_\beta}. \tag{8}$$

For our stress relaxation test, the stretch λ is fixed. With knowing the material parameters: μ, μ_α, μ_β, τ_1 and τ_2, a combination of Eq. (6), (7), and (8) allows us to predict the stress relaxation with time, namely, $\sigma(t)$. Likewise, we can obtain those material parameters by fitting the theoretical predictions with the experiment results.

5 Results & discussion

5.1 Viscoelasticity of covalently crosslinked PAAm gel

When AAm monomers are dissolved in water, they form an elastic covalently crosslinked PAAm hydrogel network (Fig. 3.a). However, upon the immersion of PAAm chains in a viscous alginate solution, the formed hydrogel network (Fig. 3.b) is expected to behave differently under compressive strains.

Upon the application of a constant compressive strain, the covalently crosslinked PAAm gel experiences hyperplastic behavior with minimum relaxation over a long period of time,

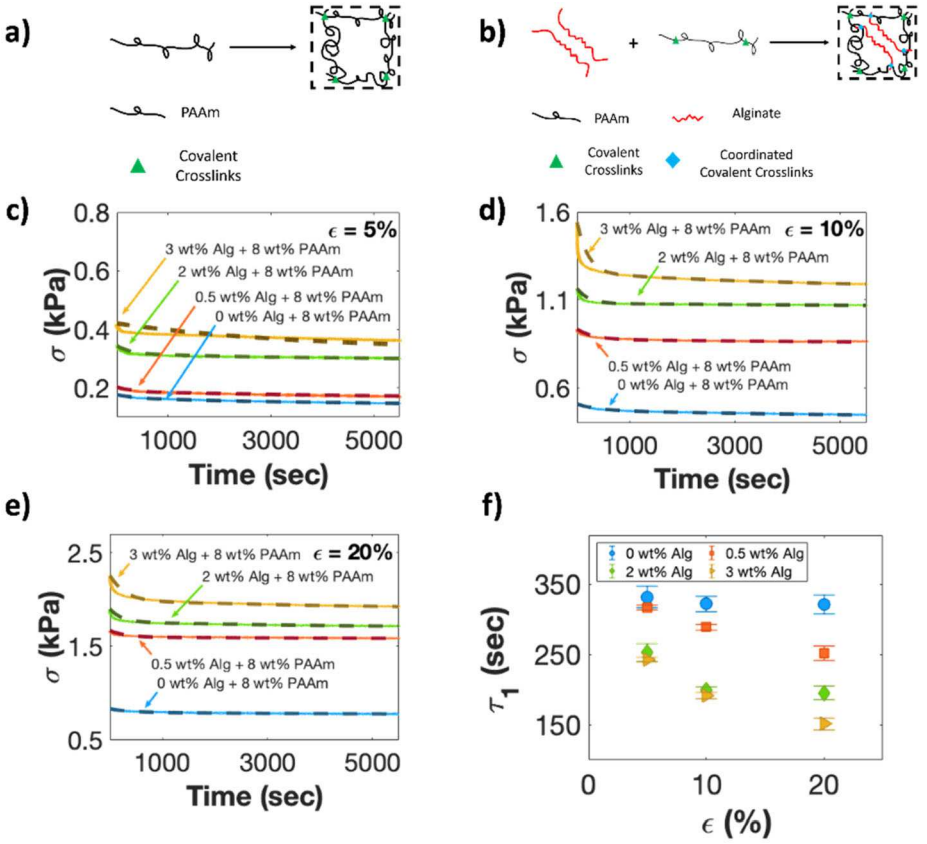

Fig. 3 A hydrogel with the molecular structure seen in **(a)** is developed when AAm monomers are crosslinked to form an elastic network composed of PAAm chains. When these chains are immersed in a viscous solution of uncrosslinked alginate chains **(b),** both covalent (green triangles) and coordinated covalent bonds (blue diamonds) form within this network. To determine how the alginate viscosity will affect the viscoelastic behavior of the gel, we designed networks with varying concentrations of alginate and observed the relaxation behavior under constant compressive strain. By increasing the viscosity of the alginate, and when compared to the single network PAAm gel (0 wt% Alg), viscoelastic behavior is observed at $\varepsilon = 5\%$ **(c)**, $\varepsilon = 10\%$ **(d)** and $\varepsilon = 20\%$ **(e)**. Additionally, an increase in stiffness is observed due to the interaction between the two polymer chains. Using the Gent model fitting results (dashed lines in c, d, and e), we plot primary relaxation time (τ_1) as a function of compressive strain, which shows faster relaxation time with increased alginate viscosity **(f)** (Color figure online)

as seen in the stress vs. time curves in Fig. 3. We expect this type of elastic behavior because the permanently crosslinked polymer network is immersed in water which has very low viscosity. However, under the same compressive strain, and as more alginate solution is added into the network, obvious viscoelastic behavior is observed. At 5% compression (Fig. 3.c), the PAAm gel (0 wt% Alg) has a maximum stress (σ_{max}) value of 0.177 kPa and an equilibrium stress (σ_0) value of 0.136 kPa, confirming minimal relaxation behavior. However, when exposed to the same compressive strain of 5%, the PAAm network immersed in 3 wt% alginate solution starts with a σ_{max} value of 0.42 kPa and reaches a σ_0 of 0.32 kPa at the end of the test.

In this case, the relaxed stress ($\Delta\sigma$) of 0.1 kPa is generated by the viscous alginate solution, while the PAAm gel dissolved in water had $\Delta\sigma$ of 0.041 kPa, confirming how the two gels behave differently under the same constant compressive strain. As higher compressive strains are applied to the gels, the effect of alginate viscosity on the viscoelastic behavior of the gels becomes more apparent. For example, when the applied compressive strain is equal to 10% (Fig. 3.d), the PAAm gel still behaves elastically with a σ_{max} that is equal to 0.51 kPa and σ_0 of 0.44 kPa ($\Delta\sigma = 0.07$ kPa). We compare this to the behavior of the PAAm gel immersed in 2 wt% alginate under the same compression and find that the $\Delta\sigma$ is equal to 0.106 kPa. This is also true when a 20% compressive strain is applied (Fig. 3.e), and the viscoelastic behavior is observed even with the PAAm gel immersed in as little as 0.5 wt% alginate where the $\Delta\sigma$ is equal to 0.102 kPa, while the pure PAAm gel still exhibits elastic behavior and has a $\Delta\sigma$ of 0.07 kPa.

To quantitatively study the dependence of the relaxation time on the applied strain and to illustrate the effect of solution viscosity on the gel's viscoelastic behavior, we fit the experimental data with the theoretical predictions. Using Eq. (6), (7), and (8) along with the assumptions discussed in Sect. 4, we can plot the stress as a function of time as predicted by the viscoelastic Gent model where the theoretical curves are shown as dashed lines in Fig. 3.c, d, and e. More importantly, these fitting curves allow us to evaluate two relaxation times: a primary relaxation (τ_1) and a secondary relaxation (τ_2), the values of which are listed in Table 1 and the Supplementary Table, respectively.

To gain deeper insight into the relaxation mechanism and how it changes with different viscosity of alginate solution, we use the fitting results and plot the primary relaxation time (τ_1) as a function of applied compressive strain in Fig. 3.f. Our calculations reveal that when PAAm is dissolved in water with 0 wt% alginate, its relaxation time remains constant as higher compressive strains are applied (Table 1). That is no longer the case when the PAAm is dissolved in a viscous alginate solution where faster relaxation times are observed at higher compression (Table 1). Interestingly, the primary relaxation time is directly correlated to the alginate solution's viscosity, where faster relaxation time is achieved as the alginate concentration is increased (Fig. 3.f, Table 1).

Because the relaxation time for the uncrosslinked alginate solution is very short (<1 s) and the PAAm gel shows negligible relaxation (Fig. 3.f), the observed decrease in relaxation with applied strain for crosslinked PAAm network immersed in viscous alginate solution is associated with the additional interactions between PAAm and alginate polymer.

Additionally, it is noted that the equilibrium modulus (μ) of the gel also increases with the increased concentration of alginate polymer in the solution, as shown in Table 2 and the stress vs. time curves in Fig. 3. Apparently, the increase of the equilibrium modulus of the gel cannot be caused by the increase of the viscosity of the solution in the gel. However, such modulus increase can be attributed to the interaction between the amine groups on the PAAm and carboxyl groups on the alginate, which results in the formation of coordinated covalent bonds (illustrated by blue diamonds in Fig. 3.b) (Sun et al. 2012; Agulhon et al.

Table 1 The primary relaxation time (τ_1) of all the tested gels obtained from theoretical fitting of the rheological model using experimentally collected data and the standard deviation values based on 3 tested samples per gel. As seen in Fig. 3.f, and when compared to the relaxation time of the single network PAAm gel, the addition of uncrosslinked alginate into the PAAm network results in decreasing the relaxation time under the same compressive strain. Furthermore, as the concentration of the alginate chains is increased within the PAAm network, a significant reduction in the relaxation time is observed at higher compressive strains associated with the additional interactions between the PAAm and alginate polymer chains

Primary Relaxation Time (τ_1, sec)			
Hydrogel	5% $\varepsilon_{Compression}$	10% $\varepsilon_{Compression}$	20% $\varepsilon_{Compression}$
0 wt% Alg + 8 wt% PAAm	332.30 ± 15.6	322.18 ± 11.1	321.30 ± 13.6
0.5 wt% Alg + 8 wt% PAAm	317.41 ± 3.35	289.07 ± 4.35	251.61 ± 10.38
2 wt% Alg + 8 wt% PAAm	253.26 ± 12.28	200.01 ± 4.24	195.47 ± 9.49
3 wt% Alg + 8 wt% PAAm	242.50 ± 3.42	191.40 ± 4.82	151.43 ± 8.92
2 wt% Alg	343.89 ± 86.2	221.95 ± 30.3	66.93 ± 25.41
PAAm-Alg Double Network	596.59 ± 80.2	232.14 ± 79	142.38 ± 29.8

2012; Fiorillo and Galbraith 2004). By increasing the amount of alginate solution in the gel, we statistically increase the interaction between the alginate and crosslinked PAAm, which results in the formation of more coordinated covalent bonds within the gel and consequently increases its equilibrium modulus and crosslink density along with the number of chains per unit volume.

The effect of the coordinated covalent bonds can be quantitatively evaluated through the equilibrium moduli reported in Table 2, where the equilibrium shear modulus of the hydrogel can be estimated using Eq. (9) as follows:

$$\mu = Nk_BT, \tag{9}$$

where N is the number of chains per unit volume of the gel, k_B is the Boltzmann constant, and T is the absolute temperature. For a purely elastic hydrogel (0 wt% Alg + 8 wt% PAAm), $\mu = 1.20$ kPa. When 0.5 wt% alginate is added, the modulus equals 2.08 kPa, which increases the equilibrium modulus ($\Delta\mu$) by 0.88 kPa.

The addition of 2 wt% and 3 wt% alginate results in a $\Delta\mu = 1.55$ kPa and 1.64 kPa, respectively. The results are plotted in Fig. 4, and based on these calculations, we can estimate that a 1% increase in alginate concentration results in increasing the equilibrium modulus by 0.64 kPa, which can be attributed to an increase in coordinated covalent bond density within the hydrogel network.

Using Eq. (9) and given that $k_BT = 4.10 \times 10^{-21}$ J, we can estimate that, on average, a 1% increase of alginate results in increasing the number of polymer chains by $1.55 \times 10^{23}/\text{m}^3$.

5.2 Ionically crosslinked alginate gel

When the alginate is mixed with water in the presence of divalent metal ions such as Ca^{2+}, it forms egg-box structured crosslinkers (Agulhon et al. 2012). Upon applying constant compressive strain, the ionic bonds experience unzipping under compression for a long period of time (Fig. 5.a). To determine the force-dependent relaxation behavior of the gel, we measure the stress relaxation of the gel under four different compressive strains (Fig. 5.b). To better reveal the force-dependent relaxation dynamics observed in the experiments, we normalize

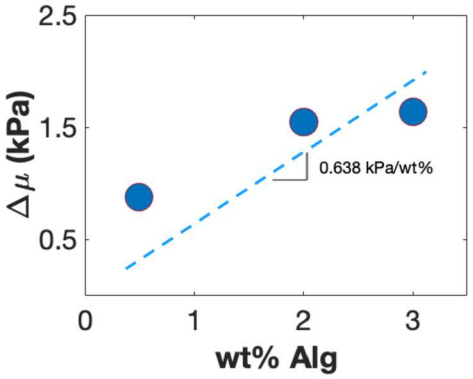

Fig. 4 The Change in equilibrium modulus ($\Delta\mu$) as a function of weight percentage alginate

Table 2 The shear moduli μ, μ_α and μ_β for all the tested gels were obtained based on the theoretical fitting of the rheological model using experimentally collected data. When the AAm monomers are immersed in the viscous alginate solution, an increase in the values of the equilibrium modulus μ is observed as a function of the alginate concentration, which can be attributed to the formation of coordinated covalent bonds. Finally, and compared to single network gels, the double network gel has significantly larger moduli due to the formation of ionic, covalent, and coordinated covalent bonds within its network

Hydrogel	μ (kPa)	μ_α (kPa)	μ_β (kPa)
0 wt% Alg + 8 wt% PAAm	1.20	0.08	0.13
0.5 wt% Alg + 8 wt% PAAm	2.08	0.14	0.17
2 wt% Alg + 8 wt% PAAm	2.75	0.23	0.12
3 wt% Alg + 8 wt% PAAm	2.84	0.68	0.25
2 wt% Alg	2.22	1.38	1.51
PAAm-Alg Double Network	4.12	2.85	1.82

the relaxation stress as:

$$\sigma_{Normalized} = \frac{\sigma\,(t) - \sigma_0}{\sigma_{max} - \sigma_0} \tag{10}$$

where $\sigma\,(t)$ is the relaxation stress at time t, σ_0 is the equilibrium stress which is obtained at $t = 10{,}800$ seconds and σ_{max} is the initial stress when relaxation starts ($t = 2$ seconds), which is the value of the maximum compressive stress as defined in the previous section. The normalized stress as a function of time is plotted in Fig. 5.c and clearly illustrates accelerated relaxation behavior at higher strain.

As stated in Sect. 5.1, we can plot the stress as a function of time as predicted by the Gent model, where the theoretical curves are shown as dashed lines in Fig. 5.b. In doing so, we obtained the primary (τ_1, Table 1) and secondary relaxation time (τ_2, Supplementary Table) along with the values of μ, μ_α and μ_β (Table 2). According to fitting results of the rheological model, the primary relaxation time decreases with increased compressive strain (Fig. 5.d, Table 1). At the lowest compressive strain of 5%, the gel's relaxation time was 343.89 seconds, whereas at the highest compressive strain of 20%, the gel underwent relaxation within 66.93 seconds, which is 80.5% faster.

We next correlate the measured stress relaxation kinetics to the ionic debonding process. Without the application of an external force, we assume the time needed for the ionic

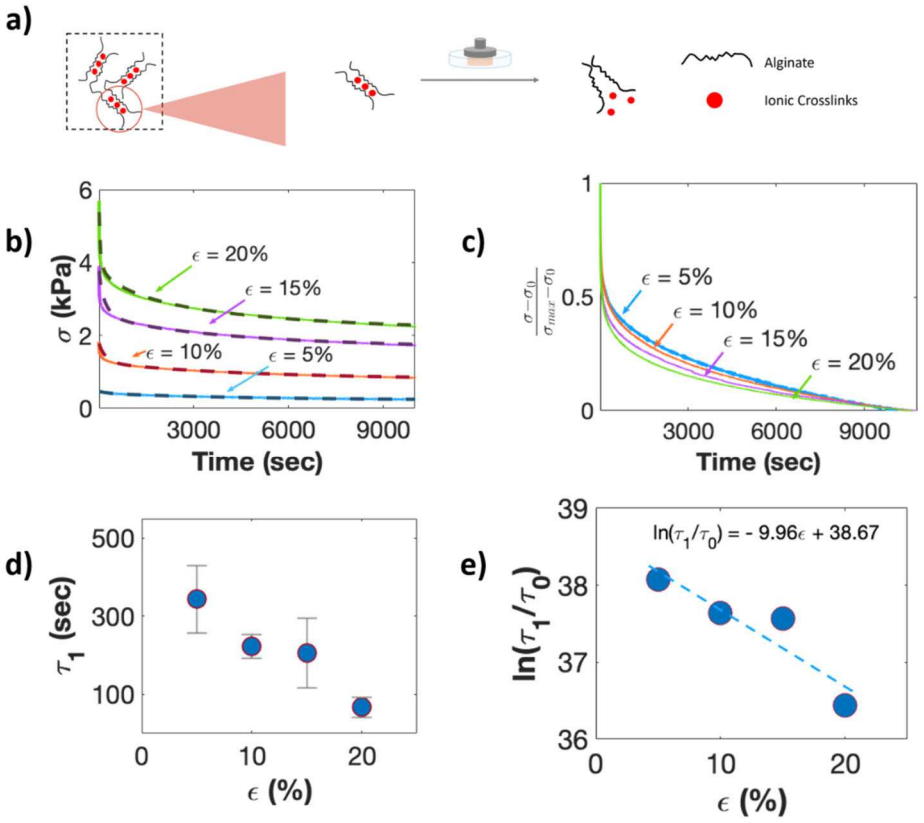

Fig. 5 The stress relaxation mechanism of ionically crosslinked alginate hydrogel due to the unzipping of its ionic bonds in the presence of constant compressive strain is illustrated in **(a)**. The stress relaxation behavior was observed under 5%,10%, 15%, and 20% compressive strain based on stress vs. time **(b)**, where the solid line shows experimental data while the dashed line represents Gent model fitting. Normalized stress is plotted as a function of time **(c),** where strong force-dependent viscoelastic behavior is observed. The Gent model fitting results were used to plot the primary relaxation time (τ_1) and $\ln(\tau_1/\tau_0)$ as a function of applied compressive strain in **(d)** and **(e)**, respectively, where $\tau_0$is the inverse of the average atomic frequency and is equal to 10^{-14} seconds (Color figure online)

debonding can be described using the primary relaxation time (τ_1) as:

$$\tau_1 = \frac{1}{\nu}\exp(\frac{E_a}{k_B T}), \tag{11}$$

where ν is the average atomic frequency, the typical value of which is 10^{14} Hz, E_a is the dissociation energy, k_B is Boltzmann's constant (1.38×10^{-23} J/K), and T (300 K) is the absolute temperature.

We assume that the stress relaxation measured in the alginate hydrogel stems from the ionic debonding. When a polymer chain is subject to force f, the ionic debonding time can be modified as:

$$\tau_1 = \frac{1}{\nu}\exp\left(\frac{E_a}{k_B T}\right)\exp\left(\frac{f\Delta_a}{k_B T}\right), \tag{12}$$

where Δ_a is the activation length. By re-arranging Eq. (12), we obtain the following linear equation:

$$\ln\left(\frac{\tau_1}{\tau_0}\right) = \frac{E_a}{k_B T} - \Psi\varepsilon, \tag{13}$$

where $\tau_0 = 1/\nu = 10^{-14}$ seconds and $\Psi = \frac{K\Delta_a}{k_B T}$, with the assumption $f = K\varepsilon$.

In Fig. 5.e, we plot $\ln\left(\frac{\tau_1}{\tau_0}\right)$ as a function of the applied compressive strain where linear fitting is used to determine the values of $\frac{E_a}{k_B T} = 38.67$ and $\Psi = 9.96$ based on the y-intercept and slope. We can calculate the dissociation energy E_a to be 96.4 kJ/mol. This is consistent with previous studies, which report values that range from 93.5 to 102.3 kJ/mol (Agulhon et al. 2012; Hashemnejad and Kundu 2019; Fang et al. 2007).

We can link the force f that one chain experiences, Young's modulus, and the applied strain based on the eight-chain model (Cioroianu et al. 2016):

$$f = El_0^2 \frac{\sqrt{3}}{4}\varepsilon, \tag{14}$$

where $E = 0.013$ MPa and is Young's modulus, ε is the applied compressive strain, and l_0 is the mesh size of the polymer network (Campbell et al. 2019). Based on the definition of Ψ, we have:

$$\Psi = \frac{\sqrt{3}El_0^2\Delta_a}{4k_B T}. \tag{15}$$

Built on previous studies, we put the mesh size of the alginate gel to be 50 nm, and by using Eq. (14), we find that the activation length $\Delta_a \cong 1.85$ nm, and this is comparable to the size of a G-Block, which forms an ionic bond with the Ca^{2+} in the alginate gel (Agulhon et al. 2012).

5.3 Crosslinked PAAm-alginate double network hydrogel

Double network gels have been recently intensively explored to achieve superior mechanical properties. A representative double network gel is formed by combing these two polymers (Fig. 6.a) with covalent (green triangles) and ionic (red circles) bonds in addition to the coordinated covalent bonds (blue diamonds) that form due to chain interaction as discussed in Sect. 5.1. Under three different compressive strains (Fig. 6.b), the double network hydrogel behaves similarly to the single network alginate gel with a noticeable change in relaxation behavior at higher strain, as shown in Fig. 6.c, where normalized stress is plotted as a function of time. The results indicate that the stress relaxation in a double network gel is also associated with unzipping ionic bonds within the gel's network.

Like what we did previously, fitting data of the rheological model (dashed lines in Fig. 6.b) were used to determine the two relaxation times as a function of the applied strain (Fig. 6.d, Table 1, Supplementary Table), and the results confirm the presence of strong force-dependence behavior due to the alginate ionic bonds that exists within the hydrogel's double network.

Using Eq. (13) and the concept of microscopic force sensitivity explained in Sect. 5.2, the value of Ψ for the double network hydrogel was found to be equal to 8.92 (Fig. 6.e), which is smaller than the value for single network alginate. Such difference is mainly because of

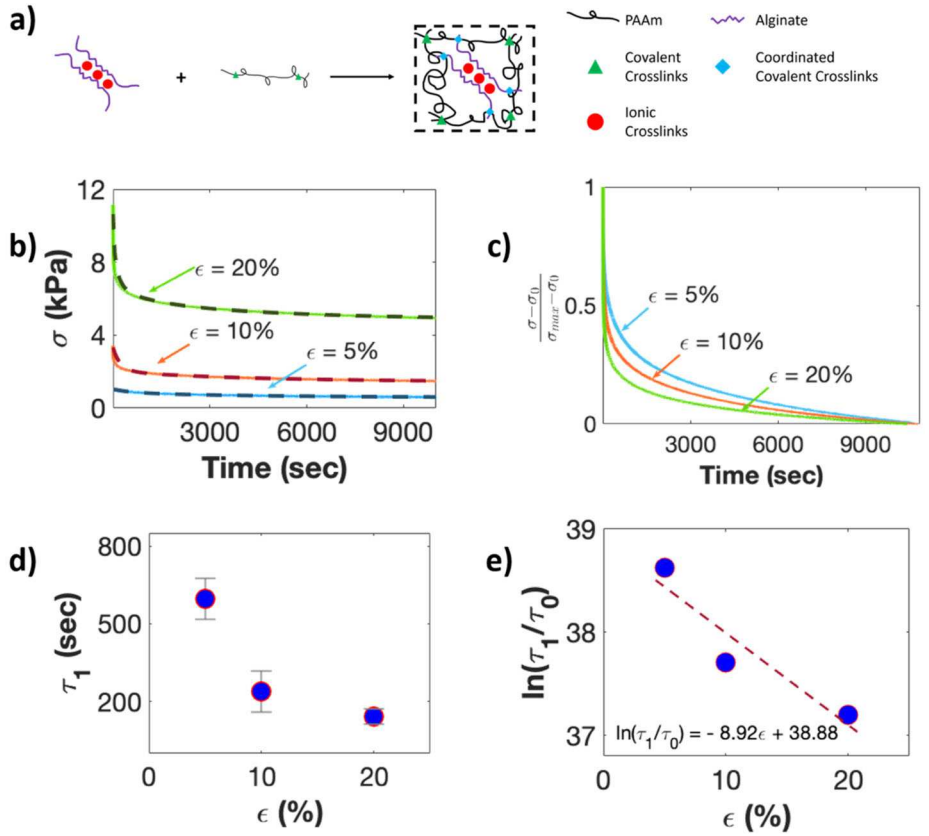

Fig. 6 The two single networks were combined to create a double network hydrogel with ionic bonds and the two types of covalent bonds previously discussed within its network **(a)**. The stress relaxation behavior of the double network hydrogel was observed under 5%, 10%, and 20% compressive strain based on stress vs. time **(b)**, where a significant increase in stiffness was observed due to the formation of multiple bonds within the gel. At higher compressive strains, we observe strong force-dependent viscoelastic behavior when normalized stress is plotted as a function of time **(c)**. The Gent model fitting results were used to plot the primary relaxation time (τ_1) and $\ln(\tau_1/\tau_0)$ as a function of applied compressive strain in **(d)** and **(e)**, respectively, where $\tau_0$is the inverse of the average atomic frequency and is equal to 10^{-14} seconds (Color figure online)

the different environment and chain topology in ionically crosslinked alginate gel and the double network gel. Although the value of Ψ is different for the two gels, the dissociation energy E_a value remains unchanged and is similarly equal to 96.9 kJ/mol for the double network gel. This is expected since the energy source comes from the ionic debonding of the alginate chains, which are present in equal amounts in both hydrogels.

Furthermore, and based on the results obtained from the Gent model, we find that the double network equilibrium modulus (μ) was equal to 4.12 kPa, which is 17% higher than the addition of the single network module (Table 2), and this again can be explained by the formation of the coordinated covalent bonds between the alginate and PAAm polymer chains as described previously.

6 Conclusions

Hydrogels have been used in many applications within the biomedical field, active devices, and soft robots; however, many potential applications can be unlocked by learning how to tune their properties to meet specific requirements for unique applications.

With this aspiration in mind, we systematically investigated how to tailor the viscoelastic behavior of covalently crosslinked PAAm networks by increasing the viscosity of the aqueous solution in which the polymer network is immersed. Our results have shown that when AAm monomers are dissolved in water, the PAAm hydrogel behaves elastically under compressive strain and experiences minimal stress relaxation. However, when the same amount of AAm monomers were dissolved in a viscous alginate solution, the resulting hydrogels experienced increased viscoelastic behavior with increased alginate concentration. Through theoretical fitting of the rheological model, we reported the relaxation time and how it changes as a function of alginate concentration and applied compressive strain.

Although previous studies have assumed that the time scale associated with viscoelasticity is constant, our detailed study of the stress relaxation behavior of ionically crosslinked alginate networks and double-network hydrogels has proven otherwise. Through our experimental data and Gent model fitting, we were able to quantitatively correlate the macroscopically viscoelastic behavior of the hydrogel by confirming faster relaxation time at higher compressive strains with the microscopic ionic debonding process while using reasonable activation length Δ_a and dissociation energy E_a.

Finally, and by reporting the moduli of the six different types of hydrogels investigated in this study, we provide quantitative evidence of a widely accepted theoretical concept within the community and confirm the existence of coordinated covalent bonds that form whenever amine groups on the PAAm chains interact with the carboxyl groups on the alginate chains.

With these reported discoveries, we hope to provide the scientific community with a methodology to develop hydrogels with tunable viscoelastic properties while highlighting the importance of force-dependent stress relaxation and how it is correlated with chain debonding mechanisms within the hydrogel network.

Supplementary Information The online version contains supplementary material available at https://doi.org/10.1007/s11043-023-09640-w.

Acknowledgements The authors acknowledge the support by the NSF through grant no. CMMI-2029145 and the Saudi Aramco Advanced Degree Fellowship Program.

Author contributions N.Q, H.H and C.L worked on experimental design, sample preparation and data collection. N.Q, Z.S and S.C developed theoretical model, completed all related derivations and calculations. N.Q, Z.S and S.C wrote the main manuscript text. Z.S. prepared Fig. 2. N.Q. prepared all remaining figures. All authors reviewed the manuscript.

Declarations

Competing interests The authors declare no competing interests.

References

Agarwal, P., Lee, H.P., Smeriglio, P., Grandi, F., Goodman, S., Chaudhuri, O., Bhutani, N.: A dysfunctional TRPV4–GSK3β pathway prevents osteoarthritic chondrocytes from sensing changes in extracellular matrix viscoelasticity. Nature Biomed. Eng. **5**(12), 1472–1484 (2021)

Agulhon, P., Markova, V., Robitzer, M., Quignard, F., Mineva, T.: Structure of alginate gels: interaction of diuronate units with divalent cations from density functional calculations. Biomacromolecules **13**(6), 1899–1907 (2012)

Bai, R., Yang, J., Suo, Z.: Fatigue of hydrogels. Eur. J. Mech. A, Solids **74**:337–370 (2019)

Campbell, K.T., Wysoczynski, K., Hadley, D.J., Silva, E.A.: Computational-based design of hydrogels with predictable mesh properties. ACS Biomater. Sci. Eng. **6**(1), 308–319 (2019)

Chaudhuri, O.: Viscoelastic hydrogels for 3D cell culture. Biomater. Sci. **5**(8), 1480–1490 (2017)

Chaudhuri, O., Gu, L., Klumpers, D., Darnell, M., Bencherif, S.A., Weaver, J.C., Huebsch, N., Lee, H.P., Lippens, E., Duda, G.N., Mooney, D.J.: Hydrogels with tunable stress relaxation regulate stem cell fate and activity. Nat. Mater. **15**(3), 326–334 (2016)

Cioroianu, A.R., Spiesz, E.M., Storm, C.: Disorder, pre-stress and non-affinity in polymer 8-chain models. J. Mech. Phys. Solids **89**, 110–125 (2016)

Drozdov, A.D., Kalamkarov, A.L.: A constitutive model for nonlinear viscoelastic behavior of polymers. Polym. Eng. Sci. **36**(14), 1907–1919 (1996)

Fang, Y., Al-Assaf, S., Phillips, G.O., Nishinari, K., Funami, T., Williams, P.A., Li, L.: Multiple steps and critical behaviors of the binding of calcium to alginate. J. Phys. Chem. B **111**(10), 2456–2462 (2007)

Fiorillo, A.A., Galbraith, J.M.: A valence bond description of coordinate covalent bonding. J. Phys. Chem. A **108**(23), 5126–5130 (2004)

Green, M.S., Tobolsky, A.V.: A new approach to the theory of relaxing polymeric media. J. Chem. Phys. **14**(2), 80–92 (1946)

Guimarães, C.F., Gasperini, L., Marques, A.P., Reis, R.L.: The stiffness of living tissues and its implications for tissue engineering. Nat. Rev. Mater. **5**(5), 351–370 (2020)

Hashemnejad, S.M., Kundu, S.: Rheological properties and failure of alginate hydrogels with ionic and covalent crosslinks. Soft Matter **15**(39), 7852–7862 (2019)

Ligia, G., Deodato, R.: Viscoelastic behavior of polymers. In: Physicochemical Behavior and Supramolecular Organization of Polymers. Springer, Dordrecht (2009)

Long, R., Mayumi, K., Creton, C., Narita, T., Hui, C.Y.: Time dependent behavior of a dual cross-link self-healing gel: theory and experiments. Macromolecules **47**(20), 7243–7250 (2014)

Mayumi, K., Marcellan, A., Ducouret, G., Creton, C., Narita, T.: Stress–strain relationship of highly stretchable dual cross-link gels: separability of strain and time effect. ACS Macro Lett. **2**(12), 1065–1068 (2013)

Meng, F., Pritchard, R.H., Terentjev, E.M.: Stress relaxation, dynamics, and plasticity of transient polymer networks. Macromolecules **49**(7), 2843–2852 (2016)

Nakayama, A., Kakugo, A., Gong, J.P., Osada, Y., Takai, M., Erata, T., Kawano, S.: High mechanical strength double-network hydrogel with bacterial cellulose. Adv. Funct. Mater. **14**(11), 1124–1128 (2004)

Nam, S., Hu, K.H., Butte, M.J., Chaudhuri, O.: Strain-enhanced stress relaxation impacts nonlinear elasticity in collagen gels. Proc. Natl. Acad. Sci. **113**(20), 5492–5497 (2016)

Shen, T., Song, Z., Cai, S., Vernerey, F.J.: Nonsteady fracture of transient networks: the case of vitrimer. Proc. Natl. Acad. Sci. **118**(29), e2105974118 (2021)

Storm, C., Pastore, J.J., MacKintosh, F.C., Lubensky, T.C., Janmey, P.A.: Nonlinear elasticity in biological gels. Nature **435**(7039), 191–194 (2005)

Sun, J.Y., Zhao, X., Illeperuma, W.R., Chaudhuri, O., Oh, K.H., Mooney, D.J., Vlassak, J.J., Suo, Z.: Highly stretchable and tough hydrogels. Nature **489**(7414), 133–136 (2012)

Tang, Z., Huang, J., Guo, B., Zhang, L., Liu, F.: Bioinspired engineering of sacrificial metal–ligand bonds into elastomers with supramechanical performance and adaptive recovery. Macromolecules **49**(5), 1781–1789 (2016)

Wang, J., Cui, K., Zhu, B., Gong, J.P., Hui, C.Y., Zehnder, A.T.: Load transfer between permanent and dynamic networks due to stress gradients in nonlinear viscoelastic hydrogels. Extreme Mech. Lett. **58**, 101928 (2023)

Publisher's Note Springer Nature remains neutral with regard to jurisdictional claims in published maps and institutional affiliations.

Springer Nature or its licensor (e.g. a society or other partner) holds exclusive rights to this article under a publishing agreement with the author(s) or other rightsholder(s); author self-archiving of the accepted manuscript version of this article is solely governed by the terms of such publishing agreement and applicable law.